

Electromagnetic Absorbers based on High-Impedance Surfaces: From ultra-narrowband to ultra-wideband absorption

F. Costa^{1*}, A. Monorchio¹

¹ Department of Information Engineering, University of Pisa, Via G. Caruso, 56122 – Pisa, Italy

*corresponding author: filippo.costa@iet.unipi.it

Abstract

Different electrically-thin absorbing designs based on High-Impedance Surfaces (HIS) are presented and classified on the basis of the nature of loss. HIS structures allow achieving absorption by exploiting either dielectric or ohmic (resistive) losses. The former ultra-narrowband absorption phenomenon can be obtained by employing dielectric losses of commercial substrates. The resonant structure, often referred to as Perfect Metamaterial Absorber, usually comprises a metallic frequency selective surfaces located above a ultra-thin grounded dielectric substrate. The metamaterial absorber is also angularly stable because of its reduced thickness. Alternatively, if a loss component is introduced in the frequency selective surface located in front of the grounded dielectric substrate both narrowband and wideband absorbing structures can be designed.

1. Introduction

Recent developments in the synthesis of metamaterials has generated a great interest on thin electromagnetic absorbing materials due to the high number of practical applications [1]–[15]. Thin absorbing structures are beneficial to reduce the radar signature of targets [1]–[3], to synthesize power imaging devices [8], [9] or to improve the electromagnetic compatibility of electronic devices [15]. A wide operating bandwidth is one of the main requirements across the microwave range but frequency selective ultra-narrowband absorbing structures are desirable in THz range to design novel photodetectors [9], microbolometers [10] and phase modulators [11]. Promising and potentially revolutionary applications of metamaterial absorbers at optical frequencies regard the use of such structures as frequency selective emitters to improve the efficiency of thermophotovoltaic solar cells [12], [13].

A simple structure allowing the synthesis of both ultra-narrowband, narrowband, wideband and ultra-wideband electrically-thin absorbers is a High-Impedance Surface (HIS) [16]. The absorbing panel consists of a frequency selective surface over a thin grounded dielectric slab. As the suitable amount of loss is introduced in the resonant structure, a perfect absorption can be achieved at a single frequency or across a large band.

Aim of this paper is to introduce a classification of different absorbing configurations attainable by exploiting the properties of HIS structures. Ultra-narrowband absorption can be performed by exploiting dielectric losses of the commercial substrates only. This kind of structures are frequently referred to as Perfect Metamaterial Absorbers

[12], [14] and are mostly investigated by physicists across THz gap and within the visible part of the electromagnetic spectrum. As the ohmic losses are introduced close to the periodic pattern with resistive sheets [16] or in the periodic pattern through lumped resistors [17], [18] or resistive inks [4], the absorption bandwidth is enlarged. The bandwidth can be both narrow or wide depending on the number of parallel resonances (inductive-capacitive impedances connected in parallel) involved in the design. Resonances can be introduced both by designing a single resonant [4] or multi-resonant [19] FSS elements and by stacking more FSS layers [5].

2. Problem formulation

A 3D sketch of the analyzed absorbing structure is reported in Figure 1. Some of the most common periodic elements are reported in the same figure. The analyzed structure is basically a subwavelength resonant cavity characterized by an input impedance approaching to infinite and a reflection phase crossing zero at the resonance [20], [21]. The amount of power absorbed by the resonant cavity at the resonance is determined by the value of the real part of the input impedance since the imaginary part of the input impedance of a lossy structure is close to zero at the resonance. The magnitude of the reflection coefficient of HIS at normal incidence approximately reads:

$$|\Gamma| \approx \frac{\operatorname{Re}\{Z_{HIS}\} - \zeta_0}{\operatorname{Re}\{Z_{HIS}\} + \zeta_0} \quad (1)$$

where Z_{HIS} represents the input impedance of the absorbing HIS structure and ζ_0 is the characteristic impedance of free space at normal incidence. The input impedance of the HIS structure Z_{HIS} is equal to the parallel connection between the two complex impedances Z_{FSS} and Z_d which represent the FSS impedance and grounded substrate impedance, respectively. The impedances of the grounded substrate and the frequency selective surface in presence of a lossless or even lossy dielectric can be computed analytically on the basis of some well justified approximations [22]. By deriving an explicit expression of the real part of the input impedance of the high-impedance surface, which is directly related to the amount of loss at the resonance, several properties of the HIS absorber having immediate practical implications can be easily extracted.

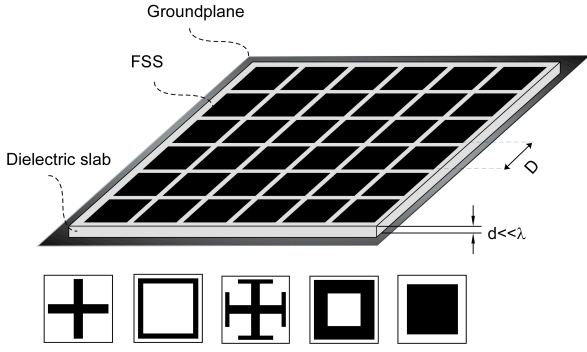


Figure 1- 3D sketch of the HIS absorber with some of the most common unit cell pattern. The periodic pattern can be metallic or resistive.

2.1. Derivation of the real part of the HIS input impedance

In order to derive the expression of the real part of the input impedance Z_H , the expressions of the grounded substrate impedance, Z_d , and the FSS impedance, Z_{FSS} , are separately derived on the basis of simple approximations and then combined. The grounded substrate input impedance is inductive until the substrate thickness is lower than a quarter wavelength whereas the periodic array on top of it is basically an FSS with a capacitive impedance before its proper resonance and with an inductive impedance after it.

Assuming $\epsilon_r' ? \epsilon_r''$, the real and the imaginary part of the input impedance can be expressed as follows [22]:

$$\begin{aligned} \text{Re}\{Z_d\} & ; \frac{\zeta_0}{\sqrt{\epsilon_r'}} \left[\frac{\epsilon_r''}{2\epsilon_r'} \text{tg} \left(k_0 d \sqrt{\epsilon_r'} \right) - \right. \\ & \left. - \left(k_0 d \frac{\epsilon_r''}{2\sqrt{\epsilon_r'}} \right) \left(1 + \text{tg}^2 \left(k_0 d \sqrt{\epsilon_r'} \right) \right) \right] \\ \text{Im}\{Z_d\} & ; \frac{\zeta_0}{\sqrt{\epsilon_r'}} \left[\text{tg} \left(k_0 d \sqrt{\epsilon_r'} \right) \right] \end{aligned} \quad (1)$$

where ζ_0 is the characteristic impedance of free space; k_0 is the free space propagation constant and d is the thickness of the dielectric substrate. The real part of the input impedance depends both on the real and imaginary part of the dielectric permittivity while the imaginary part of Z_d is almost equal to the lossless case.

The impedance of a frequency selective surface can be represented through a series LC circuit and a couple of resistors which take into account both dielectric and ohmic losses [23]:

$$Z_{FSS} = R_0 + R_D + (1 - \omega^2 LC) / (j\omega C) \quad (2)$$

where C and L represent the capacitance and the inductance of the FSS. The capacitance of an FSS printed on a dielectric substrate is computed by multiplying the unloaded capacitor

by the real part of the effective dielectric permittivity due the surrounding dielectrics.

The capacitor formed between the adjacent elements has a loss component since the electric field lines are concentrated in a lossy medium. Such loss component is readily represented by the following series resistor [22]:

$$R_D ; \frac{-\epsilon_r''}{\omega C (\epsilon_r' + 1)} \quad (3)$$

The FSS series resistor R_D is inversely proportional to the FSS capacitance.

The ohmic resistor connected in series with the aforementioned dielectric resistor can be evaluated by weighting the classical expression of the surface resistance valid for metals or resistive inks with the ratio between metalized area and periodicity of the unit cell [4]:

$$\begin{aligned} R_o & \approx \frac{S}{A} \frac{1}{\sigma \delta} \quad \text{if } t < \delta \\ R_o & \approx \frac{S}{A} \frac{1}{\sigma t} \quad \text{if } t > \delta \end{aligned} \quad (4)$$

Where t , δ and σ represent the thickness, the skin-depth and the electrical conductivity of the metallic/resistive pattern, respectively. $S=D^2$, D is the cell periodicity and A is the surface area of the lossy element within a single unit cell. The relation (4) implies that the smaller is the scattering area, the smaller is the surface resistance leading to a certain fixed lumped resistance (same amount of loss).

If the FSS is made of copper, ohmic losses obtained according to relation (4) are generally two orders of magnitude lower than the dielectric resistor (3). Conversely, if the metal is replaced with a resistive ink, the resistor assumes values higher than the dielectric resistor. Ohmic losses comes from the currents flowing on an imperfect conductor and they are increasingly important as the working frequency raises. As matter of fact, the ohmic resistor is comparable with the dielectric one in THz range and it dominates across optical regime [24].

The calculation of the unloaded capacitance can be accomplished by retrieving the reflection coefficient of a full-wave simulation [25]. As the substrate thickness is reduced (which is the case of thin metamaterial absorbers) the influence of higher-order (evanescent) Floquet modes reflected by the ground plane must be taken into account by adequately correcting the capacitance and the inductance values [25], [26].

As already remarked, the input impedance of the HIS structure Z_H is equal to the parallel connection between the two complex impedances Z_{FSS} and Z_d . At the resonance of the lossy structure, the imaginary part of the input impedance Z_H crosses the zero. After some simple algebraic operations, the real part of the input impedance Z_H at the resonance is derived [22]:

$$\text{Re}\{Z_H^{res}\} ; \frac{(\text{Im}\{Z_d\})^2}{(\text{Re}\{Z_d\} + R_0 + R_D)} \quad (5)$$

By replacing the relations (1), (3), (4) in (5), the real part of the input impedance at the resonance can be explicitly written. The expression in (5) contains all the degrees of freedom of the HIS absorber: it is a function of the FSS capacitance, of the electrical substrate thickness and of the real and imaginary part of the dielectric permittivity. $\text{Re}\{Z_d\}$ is usually much smaller than $\text{Re}\{Z_{FSS}\}$ at the main resonance of the HIS [22].

Depending of the prevalent nature of losses, different type of absorbers can be identified from relation (5):

- $R_D \gg R_O$: Ohmic losses negligible with respect to dielectric losses. The loss component is determined by the substrate properties. The substrate thickness and the FSS element needs to be chosen in order to maximize the absorption at the desired frequency. The structure is typically *ultra-narrowband*.
- $R_D : R_O$: Both ohmic and dielectric losses contribute to absorption at the resonance. The resistors' values are typically comparable in THz range because ohmic losses start to play a important role also in metallic resonant structures. They can assume comparable values also in the microwave range if low-loss substrates are employed. The structure is typically *ultra-narrowband/narrowband*.
- $R_O \gg R_D$: Ohmic losses are predominant. It is typically the case of lossy frequency selective surfaces manufactured with resistive inks or loaded with lumped resistors. Ohmic losses due to metallic patterns are predominant also in optical range even if the structure is completely metallic. The structure is typically *narrowband, wideband or ultra-wideband*.

3. Absorbing configurations

a) Ultra-narrowband and narrowband configuration

In this section the difference between HIS absorbers made up of metallic or resistive FSSs are clarified through a numerical example. In Figure 2 the dielectric and the ohmic resistance of the FSS impedance are compared with the real part of the substrate input impedance for a HIS absorber comprising a simple cross shaped FSS. The substrate is a commercial FR4. In the former case the dielectric resistor is much higher than the ohmic resistor while in the latter case the losses introduced in the periodic pattern make the ohmic resistor predominant. The use of metallic FSSs forces the choice of the substrate thickness for obtaining, according to relation (5), a value of the real part of the HIS input impedance close to the free space impedance at the resonance. The FSS element is the same in both cases but the periodicity of the metallic cross is slightly higher than the periodicity of the resistive cross in order to have absorption at the same frequency. This leads to a slightly larger capacitance for the metallic cross with respect to the resistive one.

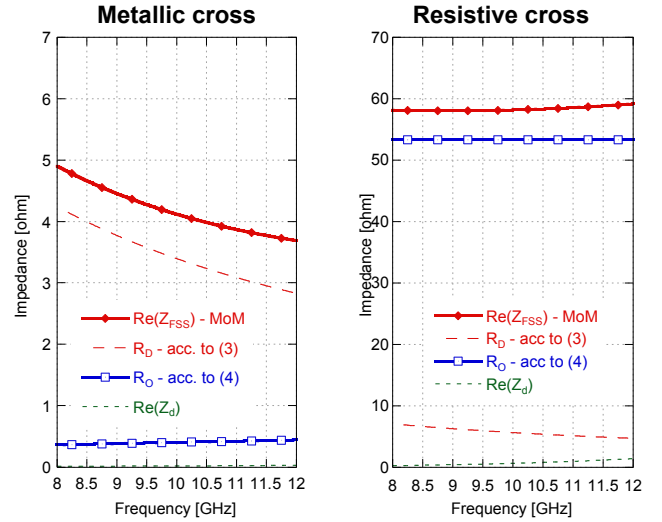


Figure 2 – Dielectric and ohmic components of the real part of the FSS impedance compared with the real part of the grounded substrate input impedance for absorbing structures comprising a metallic or a resistive FSS.

Moreover, the substrate thickness chosen for perfect absorption in the case of metallic cross is 0.5 mm while the substrate thickness for the resistive cross case is 1.6 mm. The lower substrate thickness leads to an increase of the FSS capacitance due to the influence of high-order Floquet modes [26] and as a consequence, according to (3), to a slightly lower FSS dielectric resistor.

In Figure 3 the reflection coefficient of the thin absorber comprising a metallic and a resistive cross is shown. Due to the very small substrate thickness, the absorption bandwidth of the metallic absorber is ultra-narrow. The use of resistive patterns introduces an additional degree of freedom in the relation (5). For this reason, the substrate thickness leading to a matching of the HIS input impedance with the free space impedance can be arbitrary selected. In order to maintain a perfect absorption at the resonance while the substrate thickness is increased the surface resistance of the FSS needs to be enhanced (narrowband case). The bandwidth of the absorber is directly proportional on the substrate thickness [21]. Anyway, once fixed the substrate thickness, the use of tightly coupled patch arrays allows to maximize the absorption bandwidth [4], [21]. Crosses and patches are the most representative elements since they represents the two extremity for minimizing or maximizing the bandwidth of narrowband absorbers. The reflection coefficient of a narrowband 1.6 mm thick absorber comprising a resistive patch array is also reported in Figure 3 for comparison. The electrical and geometrical parameters of the simulated structures are reported in Table 1. Other configurations were already analyzed in [4]. It is worth to point out the use of exotic elements is not necessary for obtaining a narrowband absorption. Also in the case of perfect metamaterial absorbers the FSS capacitance must be tuned for obtaining the optimal value of the dielectric resistor which fulfills the relation $\text{Re}\{Z_H^{res}\} = \xi_0$ (see (5))

and this can be simply obtained by using a variant of the

cross element, e.g. Jerusalem cross [25]. More complex FSS elements are instead very useful for achieving wideband performance.

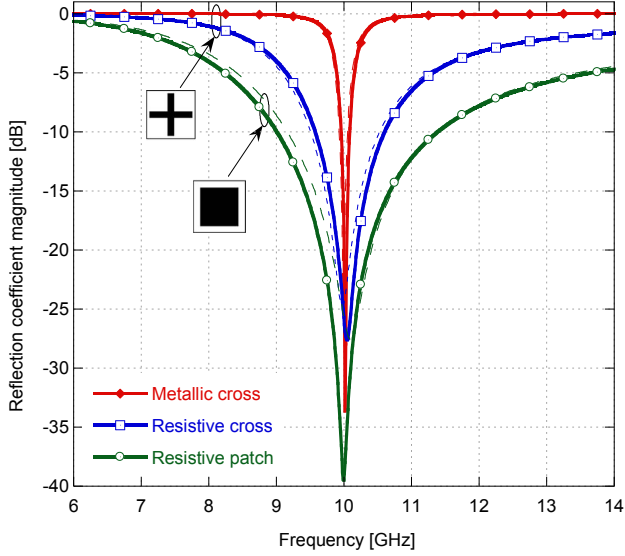


Figure 3 – Reflection coefficient of a High-Impedance Surface absorber comprising both metallic and resistive FSSs. Continuous line: MoM simulation, Dashed line: Transmission line model.

b) Wideband and ultra-wideband configuration

High-impedance surfaces can be efficiently employed also to design wideband and ultra-wideband absorbers [4], [27]. One layer wideband absorbers are efficiently synthesized through resonant elements as for instance a square loop. In [27] a capacitive method is adopted to design wideband non-magnetic absorbers employing subwavelength patch type FSSs. The methodology is very useful for multilayer lossy FSS absorbers but it is even more convenient if the number of resistive layers is larger than two. Indeed, in the latter case, the use of resonant elements would require periodicities exceeding one wavelength at maximum operating frequency leading to the onset of grating lobes. Two layers absorbers comprising resonant FSS, such as for instance a cross frame FSS [25] stacked on a ring FSS, are still more performing than capacitive designs but still require large periodicities. In Figure 4 the reflection coefficient achieved with one-layer, two-layers, three layers and four layers resistive HIS absorbers are compared. The most relevant geometrical parameters are reported in Table 2. The table reports also the minimum physical thickness for an ideal absorbing structure characterized by the same absorption properties achieved for each configuration analyzed. The limit is computed according to [28]:

$$d \geq \frac{1}{2\pi^2} \left| \int_0^\infty \ln |R(\lambda)| d\lambda \right| \quad (6)$$

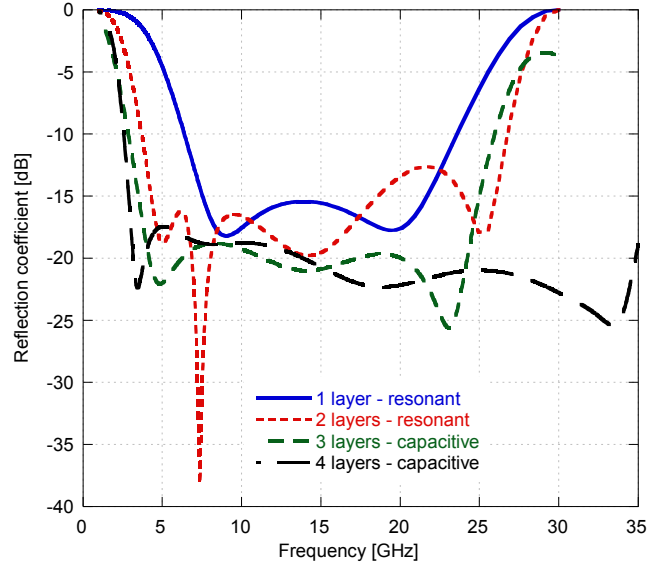


Figure 4 - Reflection coefficient of wideband 1-layer, 2-layers and 3-layers HIS absorbers. The 1-layer and 2-layers structures are synthesized by employing resonant FSS elements. The 3-layers and 4-layers structures have been presented in [27].

Table 1: Electrical and geometrical parameters of the analyzed absorbing ultra-narrowband and narrowband structures.

FSS Element	Z_s [ohm/sq]	d [mm]	D [mm]	ϵ_r
Metallic Cross	~ 0.03	0.5	8.96	4.5-j0.088
Resistive Cross	5	1.6	8.1	4.5-j0.088
Resistive Patch	40	1.6	3.7	4.5-j0.088

Table 2: Electrical and geometrical parameters of the analyzed wideband and ultra-wideband absorbing structures. The physical limit is computed according to [28].

N° layers	Thickness [mm]	Thickness over highest wavelength	Physical Limit [mm]	Pattern periodicity [mm]	FSS element
1	5	$0.12\lambda_{\max}$	4.5	11	ring
2	10	$0.14\lambda_{\max}$	9	20	ring+cross frame
3	15.1	$0.17\lambda_{\max}$	13.3	10	patch
4	14.5	$0.135\lambda_{\max}$	13.8	6.8	patch

4. Angular stability

Angular stability performance are very important for an absorbing structure. The problem can be addressed analytically with the same approach followed at normal incidence. The input impedance of the absorber can be again

computed according to relation (5) but the terms present of this relation can vary at oblique incidence in different manners for TE and TM polarizations. The ohmic resistor can be assumed angle-independent whereas the dielectric resistor varies according to the angular dependence of the capacitance [23].

So called perfect metamaterial absorbers are characterized by a very high angular stability [12] which mainly depends on the reduced thickness characterizing the absorbing panel [23].

As the substrate thickness is increased, the angular stability of the absorbing structure clearly deteriorates. A well-known method to limit angular dependences of narrowband absorbers is the use of high-permittivity dielectric substrates but they reduces the operating bandwidth. An alternative solution is the employment of vias which allows to enlarge and stabilize the bandwidth of the absorber for oblique TM polarization [29].

Wideband absorbers optimized at normal incidence are not guaranteed at oblique incidence [4] but the use of an upper dielectric substrate is a good mean for stabilizing the absorption at oblique incidence [17]. Another very effective and quick method is the genetic optimization of the absorbing structure at different incident angles based on the equivalent circuit method [5].

5. Practical realization

Practical realization of perfect metamaterial absorbers (ultra-narrowband) is very simple and it is usually performed using standard photolithographic etching process on commercial substrates [12], [14]. Practical realization of resistive FSSs for synthesizing narrow-band, wideband and ultra-wideband absorbers are extensively reported in literature over the last few years and it is usually performed with silk printing technique through a photo etched frame [4], [18]. Realization based on physical vapor deposition (PVD) can be also performed for reducing the tolerances on the value of the surface resistance. Practical realizations based on lumped resistors have been reported in [8] and [18] to name a few.

6. Conclusions

The main properties of the electrically thin absorbers synthesized by employing opportunely designed high-impedance surfaces are discussed by recurring to a simple transmission line model. The differences between an entirely metallic absorber, typically referred to as metamaterial absorber, and HIS absorbers comprising resistive FSSs are highlighted. It is shown that dielectric losses are predominant for metamaterial absorbers while ohmic losses are the most influent in case of resistive losses. The ultra-narrowband absorption achievable with metamaterial absorbers is not appealing for application in the microwave range but its employment in THz gap and optical range is promising. Finally the properties of one layer or multi-layers wideband absorbers are presented.

References

- [1] Munk, B. A., *Frequency Selective Surfaces – Theory and Design*, John Wiley & Sons, New York, 2000.
- [2] Costa F., A. Monorchio, “A Frequency Selective Radome with Wideband Absorbing Properties” *IEEE Transaction on Antennas and Propagation*, vol. 60, no. 6, pp. 2740-2747, 2012.
- [3] Costa F., S. Genovesi, and A. Monorchio, “A Frequency Selective Absorbing Ground Plane for Low-RCS Microstrip Antenna Arrays”, *Progress In Electromagnetics Research*, vol. 126, 317-332, 2012.
- [4] Costa, F., A. Monorchio, G. Manara, “Analysis and Design of Ultra Thin Electromagnetic Absorbers Comprising Resistively Loaded High Impedance Surfaces”, *IEEE Trans. on Antennas and Propagation*, vol. 58, no. 5, pp. 1551-1558, 2010.
- [5] Kazemzadeh, A., A. Karlsson, "Multilayered Wideband Absorbers for Oblique Angle of Incidence," *IEEE Transactions on Antennas and Propagation*, vol.58, no.11, pp.3637-3646, Nov. 2010.
- [6] Costa, F., A. Monorchio, “A Frequency Selective Radome with Wideband Absorbing Properties” *IEEE Transaction on Antennas and Propagation*, vol. 60, no. 6, pp. 2740-2747, 2012.
- [7] Hong-Kyu J., J. H. Shin, C. G. Kim, "Low RCS patch array antenna with electromagnetic bandgap using a conducting polymer," *International Conference on Electromagnetics in Advanced Applications (ICEAA)*, pp.140-143, 20-24 Sept. 2010.
- [8] Yagitani, S., K. Katsuda, M. Nojima, Y. Yoshimura, and H. Sugiura, “Imaging Radio-Frequency Power Distributions by an EBG Absorber,” *IEICE Trans. Commun.*, vol. E94-B no.8 pp.2306-2315.
- [9] Maier, T. and H. Bruckl, “Wavelength-Tunable Microbolometers with Metamaterial Absorbers,” *Optics Letters* 34 (19), p.3012 (2009).
- [10] Kuznetsov, S. A., A. G. Paulish, A. V. Gelfand, P. A. Lazorskiy, V. N. Fedorin, “Bolometric THz-to-IR converter for terahertz imaging”, *Appl. Phys. Lett.* Vol. 99, 023501, 2011.
- [11] Chen, H.-T., W. J. Padilla, M. J. Cich, A. K. Azad, R. D. Averitt, and A. J. Taylor, “A metamaterial solid state terahertz phase modulator,” *Nature Photonics*, vol. 3, 148–151, 2009.
- [12] Liu, T. Tyler, T. Starr, A. F. Starr, N. M. Jokerst, and W. J. Padilla, “Taming the blackbody with infrared metamaterials as selective thermal emitters,” *Phys. Rev. Lett.* 107(4), p. 045901, 2011.
- [13] Greffet, J. , *Controlled Incandescence*, *Nature* 478 (2011) 191.
- [14] Landy, N. I., S. Sajuyigbe, J. J. Mock, D. R. Smith, and W. J. Padilla, “Perfect metamaterial absorber,” *Phys. Rev. Lett.*, vol. 100, 207402-1-207402-4, 2008.
- [15] Del Prete, P., “Reducing Cavity Resonance in Wireless Applications”, on *RF Globalnet*, May 2007.
- [16] Tsuda, Y., T. Yasuzumi, O. Hashimoto, “A Thin Wave Absorber Using Closely Placed Divided Conductive Film and Resistive Film,” *Antennas and Wireless Propagation Letters, IEEE* , vol.10, no., pp.892-895, 2011.
- [17] Munk B., P. Munk, J. Prior, “On Designing Jaumann and Circuit Analog Absorbers (CA Absorbers) for Oblique Angle of Incidence,” *IEEE Trans. on Antennas and Propagation*, vol. 55, no. 1, 2007.
- [18] Li Y. H. Zhang, Y. Fu, and N. Yuan, “RCS reduction of ridged waveguide slot antenna array using EBG radar

- absorbing material", *IEEE Antennas Wireless Propag. Lett.*, vol. 7, pp.473-476, 2008.
- [19] L. K. Sun, H. F. Cheng, Y. J. Zhou, and J. Wang, "Broadband metamaterial absorber based on coupling resistive frequency selective surface," *Opt. Express*, vol. 20, pp. 4675-4680, 2012.
- [20] Sievenpiper, D., L. Zhang, R. F. J. Broas, N. G. Alexopolous, and E. Yablonovitch, "High-impedance electromagnetic surfaces with a forbidden frequency band", *IEEE Trans. Microwave Theory Tech.*, vol. 47, no. 11, pp. 2059-2074, 1999.
- [21] Costa, F., S. Genovesi, A. Monorchio, "On the Bandwidth of High-Impedance Frequency Selective Surfaces," *IEEE Antennas Wireless & Propag. Lett.*, vol. 8, pp. 1341-1344, 2009.
- [22] Costa, F., A. Monorchio, "Closed-form Analysis of Reflection Losses of Microstrip Reflectarray Antennas" *IEEE Transaction on Antennas and Propagation*, vol. 60, no. 10, pp. 4650-4660, October, 2012.
- [23] Costa, F., S. Genovesi, A. Monorchio, G. Manara "A Circuit-based Model for the Interpretation of Perfect Metamaterial Absorbers" *IEEE Transaction on Antennas and Propagation*, under review.
- [24] Raynolds, E., B. A. Munk, J. B. Pryor and R. J. Marhefka, "Ohmic loss in frequency-selective surfaces", *Journal of Applied Physics*, vol. 93, no. 9, pp. 5346-5358, 2003.
- [25] Costa, F., A. Monorchio, G. Manara "Efficient Analysis of Frequency Selective Surfaces by a Simple Equivalent Circuit Model" *IEEE Antennas and Propagation Magazine*, vol. 54, no. 4, pp. 35-48, 2012.
- [26] Tretyakov S. A. and C. R. Simovski, "Dynamic model of artificial reactive impedance surfaces," *J. of Electromagn. Waves and Appl.*, vol. 17, no. 1, pp. 131-145, 2003.
- [27] Kazemzadeh, A. "Nonmagnetic Ultrawideband Absorber With Optimal Thickness," *IEEE Trans. on Antennas and Propagation*, , vol.59, no.1, pp.135-140, Jan. 2011.
- [28] Rozanov, K. N., "Ultimate Thickness to Bandwidth Ratio of Radar Absorbers," *IEEE Trans. on Antennas and Propagation*, vol. 48, no. 8, pp. 1230-1234, 2000.
- [29] Luukkonen O., F. Costa, C. R. Simovski, A. Monorchio, S. A. Tretyakov, "A Thin Electromagnetic Absorber for Wide Incidence Angles and Both Polarizations," *IEEE Trans. on Antennas and Propagation*, vol. 57, no. 10, 2009.